MC 0241

BOX 7 FOLDER 35

Publications, 1930 - 1931

5

CHARACTERISTICS OF SMALL GRID-CONTROLLED HOT-CATHODE MERCURY ARCS OR THYRATRONS

by

W. B. NOTTINGHAM, E.E., Ph.D.

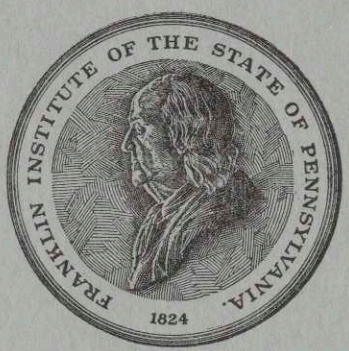

Reprinted from the Journal of the Franklin Institute,
Vol. 211, No. 3, March, 1931.

Reprinted from JOURNAL OF THE FRANKLIN INSTITUTE,
Vol. 211, No. 3, March, 1931.

CHARACTERISTICS OF SMALL GRID-CONTROLLED HOT-CATHODE MERCURY ARCS OR THYRATRONS.

BY

W. B. NOTTINGHAM, E.E., Ph.D.,

Bartol Research Fellow.

ABSTRACT.

BARTOL RESEARCH FOUNDATION

Communication No. 53.

The principle of the grid-controlled arc or thyratron is briefly described and the nominal ratings as regards filament current, maximum plate current etc. of four important thyratrons are given in table form. Methods of measuring the grid current, critical grid potential, etc., with D.C. power supply are given along with the results obtained on the General Electric Company thyratrons *FG*-17, *FG*-27 and *FG*-67. Characteristics obtained with A.C. power supply are also shown for these thyratrons and some of the relative advantages of the "phase-shift" and the "critical potential" methods of control are discussed when used in connection with photoelectric cell circuits. The A.C. measurements seem to show that a time of 10^{-3} second is required to start a thyratron. An amplifier circuit is shown by which it is theoretically possible to control a thyratron circuit using an input current to the amplifier of 10^{-11} ampere.

TABLE OF CONTENTS.

INTRODUCTION.

The name "Hot-cathode thyratron" has been given by Dr. A. W. Hull [1] to the grid controlled hot-cathode mercury arc which has recently been developed by the General Electric Company. The mechanical features and some of the electrical characteristics have been described by Hull and Langmuir,[1, 2] but many details of importance have not been published. In particular the fact that a grid current flows in the grid circuit before the discharge begins has not been emphasized. In fact it is sometimes said that the "thyratron is an electrostatically controlled arc rectifier." In a very large number of engineering applications, it is of no importance that *power* must be furnished to the grid from the control circuit, but in many problems in the physics laboratory it is important to know that power is required in the grid circuit even though it is as small as a micro-watt. This paper is therefore addressed to physicists and engineers who must interest themselves in the *detailed mechanism* of the thyratron in order to use this new and valuable thermionic device to the best advantage. It will be obvious to the reader that the experiments described here open up almost as many questions as they answer. Further experiments using the cathode-ray oscillograph, a variable frequency generator etc., may show that the interpretations of some results are not correct in every detail, but since it is not possible to carry out these more crucial tests in the near future, the results to date are being presented with the belief that they are of sufficient value to warrant their publication.

---

[1] *Gen. Elect. Rev.*, **32**, 213 and 390 (1929).
[2] *Proc. Nat. Acad. Sci.*, **15**, 218 (1929).

THE PRINCIPLE OF THE GRID CONTROLLED ARC.

The "thyratron" is a tube quite similar to the ordinary three element vacuum tube. There is a hot cathode to emit electrons, a plate to collect them and a grid between the cathode and the plate to control the flow of the electrons across the space. After evacuation, mercury which has a vapor pressure of 6×10^{-3} mm. at 40° C. is introduced as the "inert" gas * in the tubes described here. *Before the arc starts*, the grid current and plate current characteristics as a function of grid potential are identical in form with those of a gassy "vacuum" tube.[3] As the grid potential is made less and less negative, the plate current increases until, when it is about 0.2 micro-ampere, the rate of production of ions is so great that a positive ion sheath [4] is formed around the grid, neutralizing the negative charge maintained there by the bias battery. The grid then loses control and the arc starts. After the starting of the arc, the current flowing between the cathode and the plate is limited only by the external circuit conditions, assuming that the normal electron emission current from the cathode is not exceeded. The grid no longer has any appreciable control and the arc can be stopped only by lowering the plate potential below the ionization potential of the gas for a time long enough for the ions to become neutralized. When the plate potential is furnished from an alternating current source, the grid regains control during each negative half of the cycle if the frequency is not too high.

PRESENT RATINGS ON CERTAIN GENERAL ELECTRIC CO. THYRATRONS.

The characteristics which are shown in this paper must not be taken as average characteristics in any sense because only two to four samples of each type have been measured and because the manufacturing changes from time to time cause considerable alteration in such a commercial product.

In order to assist the reader in comparing the rated characteristics of the small thyratrons, Table I has been prepared

[3] Nottingham, JOURNAL OF FRANK. INST., 209, 287 (1930). See pages 291 and 295.

[4] Langmuir and Mott-Smith, "The Theory of Collectors in Gas Discharges," *Gen. Elect. Rev.*, 27, 449, 538, 616, 762, 810 (1924). *Phy. Rev.*, 28, 727 (1926).

* Thyratrons have also been made using helium, neon or argon. The characteristics of these tubes are much more independent of temperature changes.

from the technical information issued by the "Vacuum Tube Engineering Department" at Schenectady.

TABLE I.

Technical Information on Thyratrons.

Code number	*FG*-17	*FG*-27	*FG*-37	*FG*-67
Manufacturer	G. E.	G. E.	G.E.	G. E.
Designed as	Controlled Rectifier		Inverter	
Cathode				
Volts	2.5	5.0	115*	5.0
Amperes	5.0	6.0	0.2	4.5
Type	Coated filament	Indirect heat	Indirect heat	Indirect heat
Fil. heating time (min.)	0.5	5.0	5.0	5.0
Max. peak volts on plate	2500	1000	1000	1000
Max. plate current				
Instantaneous	2.0	10.0	15.0	15.0
Average	0.5	2.5	2.5	2.5
Max. tube voltage drop	24	24	24	24
Min. tube voltage drop	10	10	10	10
Temp. limits Ambient ° C.	20–50	0–50	20–50	20–50
Type of cooling	Air	Air	Air	Air
Deionization time (micro-sec.)	1000	1000	100	100
Max. freq. as rectifier	500	500	5000	5000
Gas	Mercury vapor		Mercury vapor	
Published information	GET-193*B* GEJ-278	GET-195	Technical information *FG*-37	*FG*-67 GEJ-277

* 115 volts D.C. preferred although A.C. can be used.

Thyratrons are divided into two general classes called respectively "controlled rectifier" and "inverter." These differ from each other in certain details of construction, designed to produce the most efficient operation in applications for which they are intended. The controlled rectifier is the tube which is usually used in connection with low frequency alternating plate potentials while the inverter is usually used in direct current circuits when a pulsating flow of current under the control of a subsidiary device is needed.

The three types of tubes which have been tested are the *FG*-17; *FG*-27 and *FG*-67.

CHARACTERISTICS OF AN FG-17 THYRATRON AND METHODS OF MEASUREMENT.

The alternating current or *dynamic* characteristics of thyratrons are of greater practical interest than the *static*

characteristics taken with D.C. potentials applied to the plate and the grid. The static characteristics however are of considerable theoretical interest because they can be understood in detail and they give some insight into the more complex dynamic characteristics.

(a) Static Characteristics of an FG-17 Thyratron.

The essential circuit used for the study of the static characteristics is shown in Fig. 1.

FIG. 1.

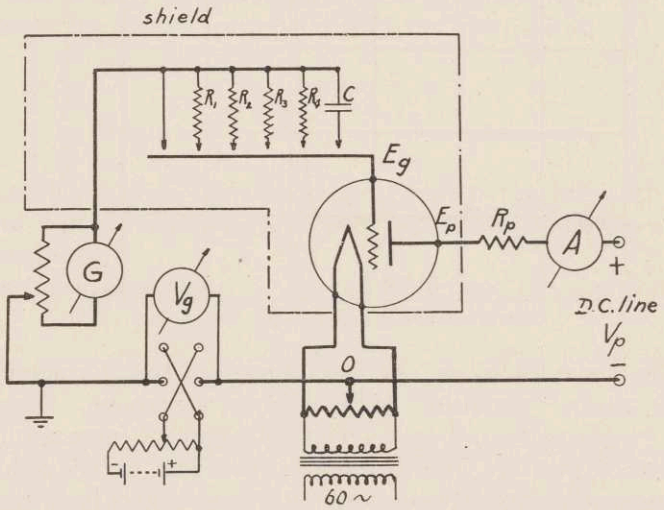

Circuit for the measurement of static characteristics of thyratrons.

In order to eliminate any possible confusion the usual conventions of vacuum tube practice will be followed.

1. All potentials are measured from the "cathode return" designated by "o" as zero.

2. The positive direction of current is that of a positive charge flowing around the circuit in the direction of the applied potential. Under this convention the flow of electrons from the filament to the plate constitutes a *positive* current.

3. The "*C*" battery or grid bias potential will be designated by V_g and the actual grid potential by E_g.

4. V_p will be used for the line potential and E_p the actual plate potential.

Figure 2 shows the grid current as a function of grid potential before the discharge begins for three different plate potentials.

FIG. 2.

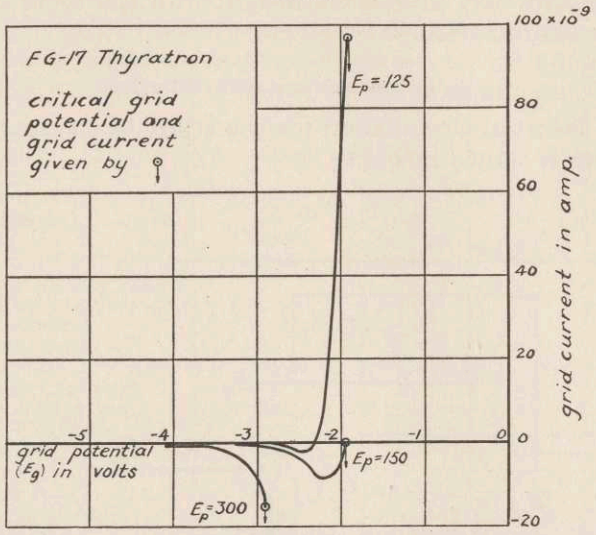

Grid current characteristic of an *FG*-17 thyratron.

The curve for $E_p = 125$ volts has all of the characteristics of the gassy "vacuum" tube referred to above. Between $E_g = -3.0$ volts and -2.4 volts the rate of increase in the number of positive ions coming to the grid exceeds that of electrons, although the actual number of each is increasing very rapidly as the grid is made less negative. Between -2.3 volts and the critical potential, the number of electrons arriving at the grid exceeds the positive ions. Since the positive ions move so much more slowly than the electrons, on account of their greater mass, a space charge is built up around the grid by this increasing number of ions coming toward it until at $E_g = -1.93$ volts an ion sheath forms around the grid; it loses control and the arc begins. With $E_p = 150$ volts the same cycle is partially completed and with $E_p = 300$ only the first stage can be observed.

An experimental difficulty in measuring these characteristics comes in on account of the fact that the current may change suddenly about a million fold as the grid potential

passes through the critical value. This can be overcome by using the following procedure.

With the galvanometer shunted the critical grid potential can be determined quite accurately since it is reproducible to within about 0.02 volt over short periods of time. With the galvanometer in the circuit the grid current can be measured safely with potentials up to within 0.1 volt of the critical value. The current at the critical grid potential can be determined by a "resistance method," that is, the critical *bias* potential V_g is determined with and without a resistance in the grid circuit. If the resistance is not too high, the grid current at the critical potential is given by equation (1),

$$\frac{V_{gr} - V_{go}}{R_g} = i_g. \tag{1}$$

Here V_{gr} and V_{go} are the critical bias potentials with and without a grid resistance respectively, and R_g is the value of the resistance.

The "grid impedance" (Z_g) can be defined by equation (2):

$$\frac{\partial i_g}{\partial E_g} \equiv \frac{1}{Z_g}, \tag{2}$$

where $\frac{\partial i_g}{\partial E_g}$ is the slope of the grid current characteristic with constant plate potential, at any particular value of grid potential.

The grid impedance (Z_g) has the dimensions of a resistance and can take on *positive* or *negative* values as in the case of the 125 volt characteristic of Fig. 2. Here it is positive at the critical value of E_g. In this case the value of i_g given by equation (1) will be independent of the value of R_g but since the grid impedance is *negative* at the critical grid potential in the 300 volt characteristic, the measured grid current using equation (1) will not be the true grid current at the critical potential unless R_g is *smaller* in magnitude than Z_g at the critical grid potential.

When R_g is greater than 10^6 ohms, it is necessary to connect a capacity of about 0.03 microfarad in parallel with the re-

sistance in order to shunt out the induced 60 cycle variations produced by the A.C. potential drop over the filament.

The negative part of the grid current characteristic was attributed above to the flow of positive ions to the grid. In order to test this assumption the plate current and the grid current were measured simultaneously as a function of the grid potential before the discharge began. The results are shown by the curve "observed grid current" of Fig. 3. The

FIG. 3.

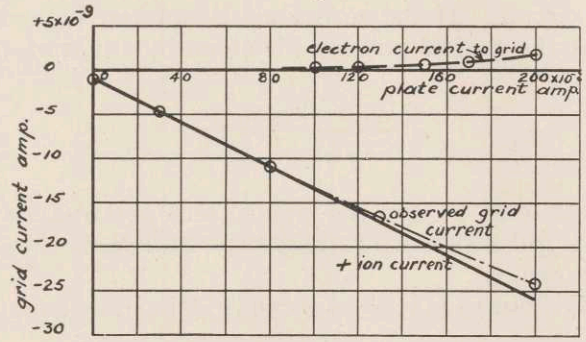

FIG. 17 thyratron with E_p = 200 volts. Positive ion current to grid is a linear function of electron current to plate.

electron current to the grid was observed with the plate potential zero. The positive ion current was found by correcting the observed current for the electron current and the result is shown by the straight line "ion current" of Fig. 3. Since the opening between the grid wires is small compared with the distance between the electrodes, the assumption is justified that the electron current to the grid is practically independent of the plate potential.

This result is consistent with the theory that a small number of electrons pass through the holes of the grid, and are accelerated in the high field between the grid and the plate. Ions are produced as a result of the impact of these high speed electrons with mercury atoms. The electrons continue to the plate and the positive ions are attracted to the grid.

A galvanometer was used to measure the plate current as the grid potential was changed for grid potentials to within 0.2 volt of the critical value. The "vacuum tube ammeter"

shown in Fig. 4 was used for the remainder of the range. With the contact "C" at "o" the bias battery V_g was adjusted to give approximately full scale deflection on the galvanometer when no current was flowing through the resistance R_p in the plate circuit of the thyratron. When a current was flowing in the thyratron, the galvanometer current measured by "G" decreased, but by adjusting the contact "C" along the re-

FIG. 4.

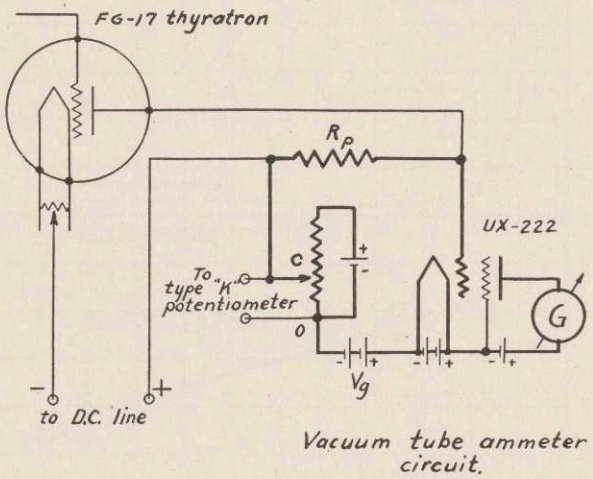

Vacuum tube ammeter circuit.

sistance, the potential difference between the grid and the filament could be returned to the original value V_g as indicated by the return of the galvanometer coil to its original deflection. The potential between "C" and "o" divided by the resistance R_p was equal to the plate current. By this method the plate current could be measured safely right up to the critical point because after the discharge began, the large potential drop over R_p simply set up a retarding potential between the grid and the filament and the current through the galvanometer fell to zero.

With these methods the plate current, the grid current and the grid potential were measured at the critical point as a function of plate potential. The results are shown by the curves of Fig. 5.

Curve *A* shows that the critical grid potential is nearly a linear function of the plate potential. From curves *B'* and *B–B* we see that the grid current is large and positive for values of plate potential less than 125 volts, but is negative and more or less independent of the plate potential for values

FIG. 5.

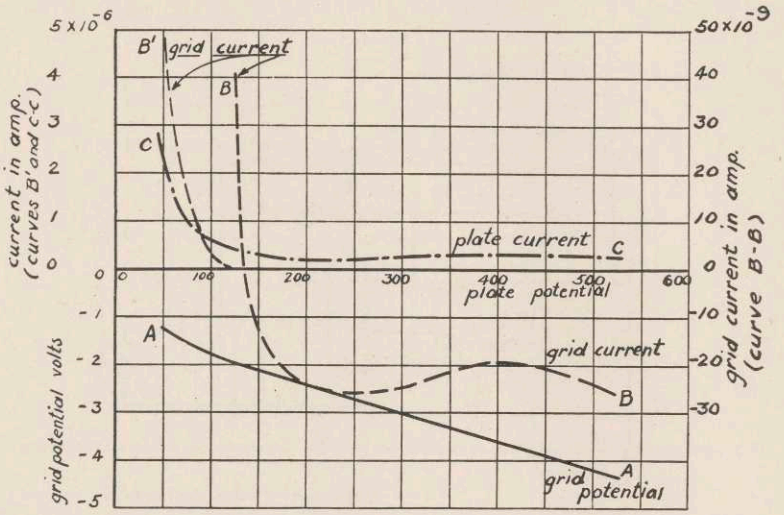

FG-17 Thyratron grid potential, grid current and plate current at critical point before discharge begins.

of 150 volts and more. In applications where grid currents of the order of 10^{-8} ampere are of importance, it is advantageous to use plate potentials in excess of 150 volts if possible. The plate current just before the discharge begins is given by curve *C–C*.

(b) Dynamic Characteristics of an FG-17 Thyratron.

The circuit used for the study of the dynamic characteristics of thyratrons is shown in Fig. 6.

The grid to filament and the grid to plate capacities are shown in schematic form by C_0 and C_1 respectively. The values of these for the *FG-17* thyratrons studied were $C_0 = 10 \times 10^{-6}$ microfarad and $C_1 = 2.0 \times 10^{-6}$ microfarad. When R_g is less than 10^6 ohms and the frequency 60 cycles, these

capacities can be neglected and, assuming no grid current the instantaneous grid potential is given by equation (3).

FIG. 6.

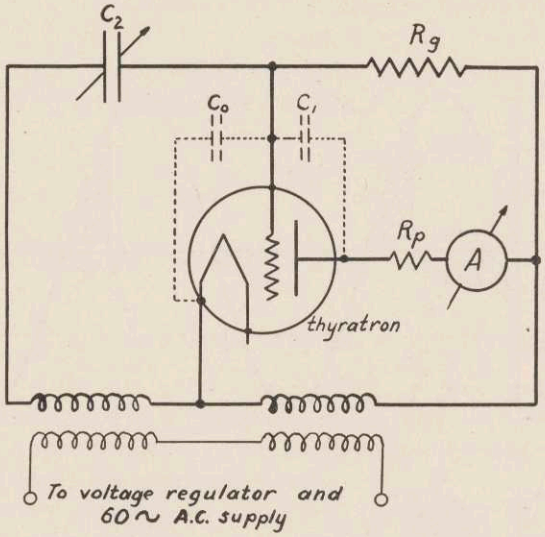

Circuit for A.C. characteristics of thyratrons.

$$E_g = V_{\max} \sin (\omega t - \alpha), \tag{3}$$

where

$$\alpha = 2 \tan^{-1} \omega C_2 R_g. \tag{4}$$

The line potential V_p is given by

$$V_p = V_{\max} \sin \omega t. \tag{5}$$

This is also equal to the plate potential E_p *before the discharge begins* but after the discharge begins the plate potential E_p is approximately constant as long as the current is flowing. Graphically these equations can be represented by the curves of case A and case B of Fig. 7 corresponding to two values of C_2.

For case A, $\omega C_2 R_g$ is 2.0 while for case B it is 0.5. The cross-hatched area is proportional to the current which flows in the plate circuit during each cycle, according to this ap-

proximate theory. The instantaneous potential (E_L) across the load resistance after the discharge begins is given by equation (6),

$$E_L = V_{\max} \sin \omega t - E'_p. \tag{6}$$

FIG. 7.

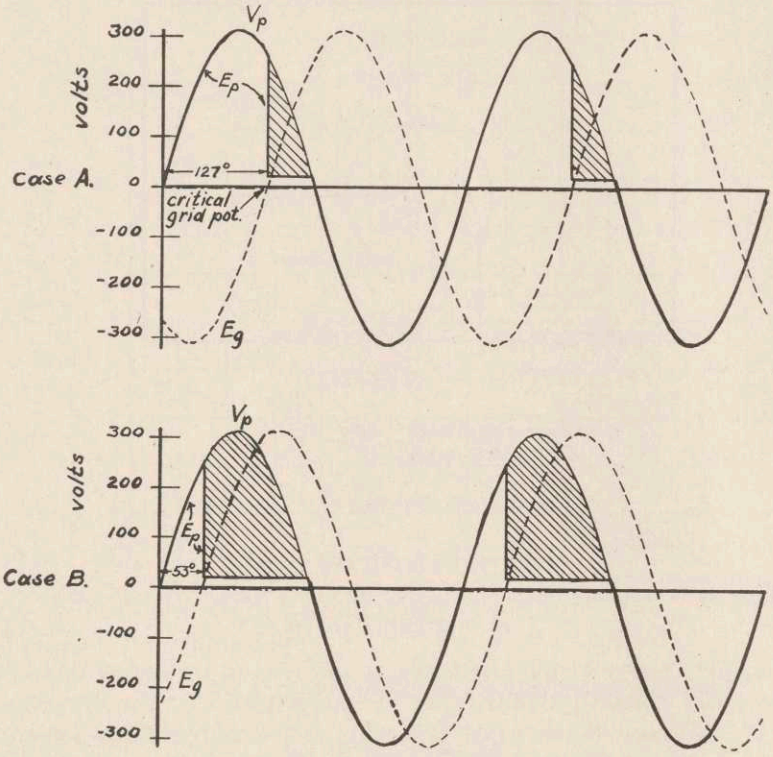

Illustration of " phase shift " method of control. Case A; $\omega C_2 R_g = 2$, and case B; $\omega C_2 R_g = 0.5$.

Where 0.707 $V_{\max}$ is the line potential as read on an A.C. voltmeter and E_p' is the potential drop over the thyratron after the discharge begins. This is seldom more than 20 volts.

The instantaneous current is given by

$$i_L = \frac{E_L}{R_p}, \tag{7}$$

and the current as read on a direct current meter is

$$I_L = \frac{1}{2\pi}\int_{\omega t=\theta}^{\omega t=\theta_0} \frac{V_{\max}\sin\omega - E_p'}{R_p}\, d\omega t. \qquad (8)$$

The upper limit of integration is obtained by putting $E_L = 0$ in equation (6) and is given by

$$\theta_0 = \pi - \sin^{-1}\frac{E_p'}{V_{\max}}. \qquad (9)$$

When integrated equation (8) becomes

$$I_L = \frac{1}{2\pi R_p}\left\{ V_{\max}(\cos\theta - \cos\theta_0) - \frac{E_p'}{57.3}(\theta_0 - \theta)\right\}, \qquad (10)$$

where θ and θ_0 are now expressed in degrees instead of radians. Here θ is approximately equal to the angle by which the plate potential *leads* the grid potential.

This very simple picture of the control of the thyratron current by the "phase shift" method, is not in exact agreement with experiment. This point is illustrated by the curves of Fig. 8 for 220 volts A.C.

In Fig. 8 the light weight solid lines V_p and I_L represent the calculated instantaneous line potential and the theoretical ammeter current as a function of the phase difference between the grid and the line potentials. For example, at $\theta = 104°$ the plate potential before the discharge begins is 300 volts and if the arc were to start at this point and continue the rest of the cycle, the plate current ammeter would read 82×10^{-3} ampere. The heavy solid curve designated by $R_g = 0.3 \times 10^6$ ohms, shows the *observed* current as a function of the phase difference between the grid and line potentials. *It is of interest to notice that no current flows in the plate circuit if the phase difference is greater than 152°* although theoretically it should be possible to get a measureable current for phase differences up to at least 176°. This difference of 24° between the calculated and observed results, seems to indicate that a time of 1.1×10^{-3} sec. is required to build the positive ion sheath around the grid and particularly around the cathode

so as to allow the full current to flow. On this basis the dotted line shown in Fig. 8 gives the calculated current assuming a time lag of 1.1×10^{-3} sec. This curve is obviously in better agreement with the observations.

FIG. 8.

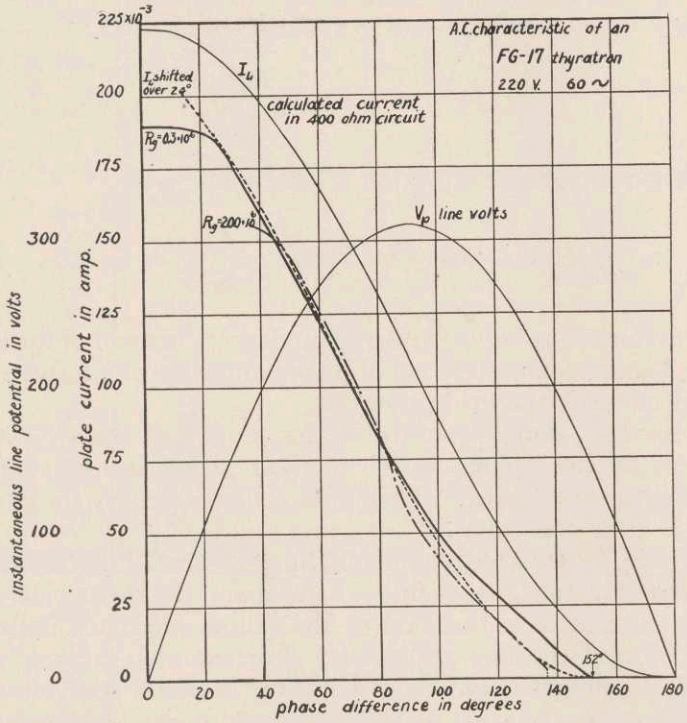

A.C. characteristic of an *FG*-17 thyratron V_p = 220 volts, 60 cycles.

This question of the time lag could be answered definitely by experiments using a cathode ray oscillograph and a variable frequency generator. Other deviations between observed and calculated results might be due to the presence of a 180 cycle component in the line voltage which could also be examined with an oscillograph.

Observed results using a resistance R_g of 10^6 ohms instead of 0.3×10^6 came so close to those shown by the solid line that it would only confuse the picture to try to show them.

With a grid resistance R_g of 200×10^6 ohms, the capacity C_2 of Fig. 6 had to be made so small that the internal capacities of the tube C_0 and C_1 could not be neglected. Hull's [1] formula for the calculation of the phase angle α for this case is given in equation (11)

$$\alpha = \tan^{-1} \frac{R_g\omega(2C_2 + C_0)}{1 + R_g^2\omega^2(C_1 - C_2)(C_0 + C_1 + C_2)}. \qquad (11)$$

The observed results shown by the "dot-dash" line of Fig. 8, indicate that with this high value of R_g the plate current starts in abruptly with a value of 4×10^{-3} ampere instead of

FIG. 9.

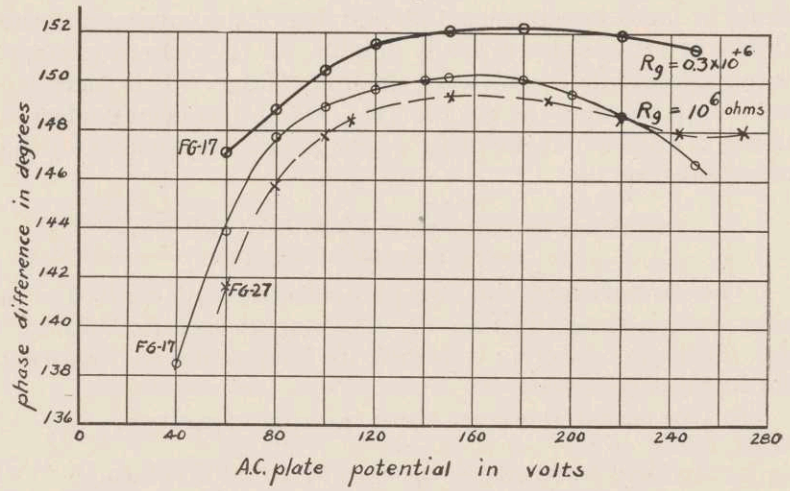

Maximum phase difference between grid and plate potentials of a thyratron for operation on 60 cycles A.C.

gradually with a value as low as 10^{-5} ampere or less as in the case of the lower grid resistance. The true phase of the grid is probably given by the current value on the solid line, showing that the grid current which has been neglected is responsible for an increase in the phase shift at the start of about 10°. The abruptness of the starting current foreshadows the result that with very high grid resistances or with small currents in photoelectric circuits, the advantages of the "phase shift" method of control as compared with the "critical potential"

method largely vanish. This point will be illustrated by experiments with photoelectric cell control of the thyratron.

In order better to understand this question of the apparent time lag in the starting of the thyratron, the critical value of the starting phase angle was measured as a function of the line voltage. For this purpose, an average current of 10^{-5} ampere in the 400 ohm plate circuit was taken as the "starting current." The results are shown in Fig. 9 by the heavy and light solid lines corresponding to grid resistances of 0.3×10^6 and 10^6 ohms respectively.

The dotted line shows the result obtained with $R_g = 10^6$ ohms on an *FG*-27 thyratron which is very similar to the *FG*-17 but of higher current carrying capacity. These curves show that the lag between the actual starting of the current and the time when it was theoretically possible for the current to start, is remarkably independent of the line voltage. It is therefore very unlikely that the grid current, which has been neglected in the calculation of the phase of the grid, is responsible for the observed time lag.

THYRATRON CONTROL WITH A PHOTOELECTRIC CELL.

(a) The Phase Shift Method.

The circuit used for the photoelectric cell control of a thyratron is shown in Fig. 10. A General Electric "*PJ*-23" gas filled photoelectric cell with its base removed was used throughout this work.

In this circuit there are three internal capacities:

1. Grid to cathode, $C_0 = 10 \times 10^{-6}$ microfarad.
2. Grid to plate, $C_1 = 2 \times 10^{-6}$ microfarad.
3. Photocell anode to cathode, $C_3 = 1.6 \times 10^{-6}$ microfarad.

When C_2 was large the maximum potential across the photoelectric cell at any time during the cycle was 78 volts. This was near the maximum which could be used on this cell with safety because of the danger of starting a discharge in the photoelectric cell.

With the photoelectric cell in the dark the capacity C_2 was increased from a very small value to 29.5×10^{-6} microfarad. This value of C_2 exactly neutralized the internal capacities C_1

and C_3 and the thyratron stopped operating. With a value of C_2 smaller than 29.5×10^{-6} microfarad the grid was practically in phase with the line potential and the maximum current flowed in the plate circuit, but with C_2 larger than 29.5×10^{-6} microfarad the grid was practically 180° out of phase with the line potential.

FIG. 10

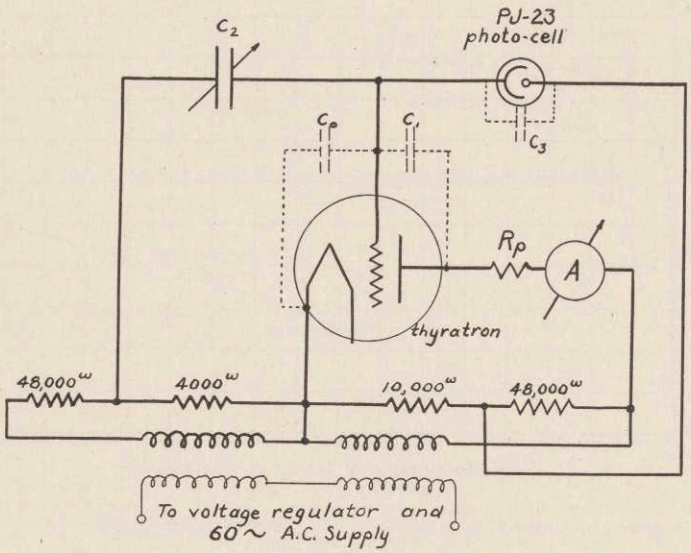

Circuit for photoelectric control of a thyratron using "phase shift" method.

The curve designated "1.05" in Fig. 11 was taken with $C_2 = 31 \times 10^{-6}$ microfarad, which is 1.05 times the neutralizing capacity. The ordinate for this graph gives the D.C. ammeter value of the plate current in the "load" circuit, while distances along the abscissa are proportional to the light intensity. The experiment was carried out by measuring the thyratron load current as a function of the lamp potential and later with a 45 volt battery and sensitive galvanometer connected to the photocell, the photoelectric current was measured as a function of lamp potential. The light intensity shown in Fig. 11 is given in terms of the photoelectric current which it produced.

When the light intensity was sufficient to give a photoelectric current of 3.5×10^{-9} ampere, the thyratron began to

pass current in slow "flashes" taking place at the rate of about ten to fifteen per second. In ear phones it sounded as though the thyratron operated for part of a cycle, and then remained off for five or six cycles. With increasing light intensity these flashes disappeared and steady operation began with a plate

FIG. 11.

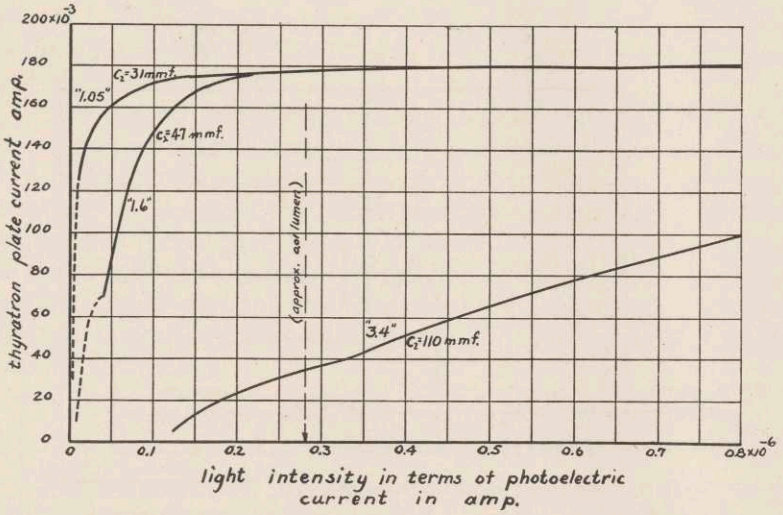

Results of photoelectric cell control of an *FG*-17 thyratron by phase-shift method. V_p = 220 volts, 60 cycles.

current of 125×10^{-3} ampere which, according to Fig. 8, corresponded to the current flowing with the grid only 60° out of phase with the line.

The increasing of C_2 to 47×10^{-6} microfarad or 1.6 times the neutralizing value, caused a decrease in the sensitivity of the system and reduced the tendency to "flash" as shown by the curve "1.6" of Fig. 11. A further increase in C_2 to 110×10^{-6} microfarad brought the thyratron current much more under the control of the light intensity with a further decrease in sensitivity.

(b) Thyratron Control with D.C. on the Photoelectric Cell.

When it is necessary to obtain very high sensitivity in the thyratron response to light intensity, without the use of an amplifier, the circuit shown in Fig. 12 can be used.

FIG. 12.

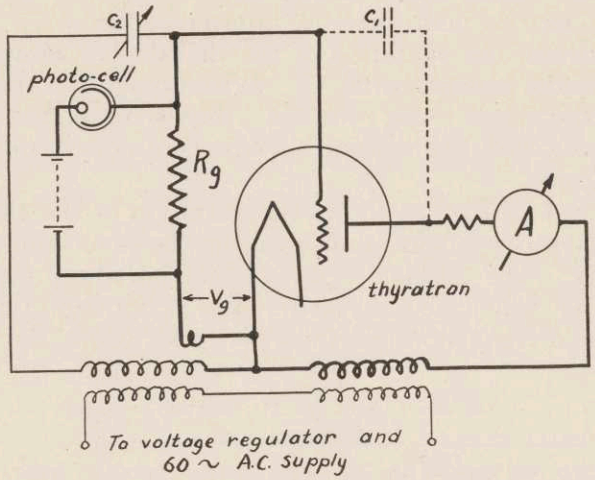

Circuit for thyratron control by photoelectric cell using critical potential method.

FIG. 13.

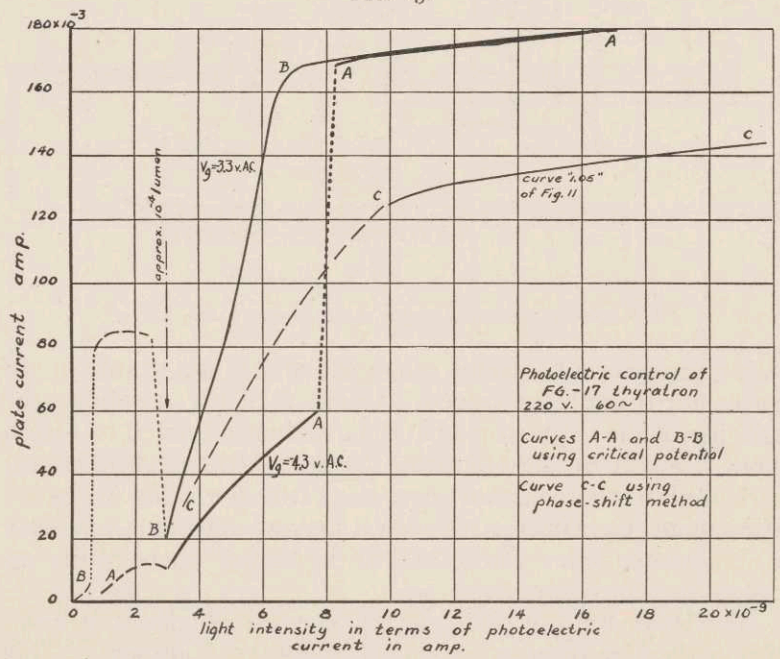

Results of photoelectric cell control of an *FG*-17 thyratron by "critical potential" method compared with "phase shift" method. Curves *A*–*A* and *B*–*B* for critical potential method and *C*–*C* for "phase shift" method. V_p = 220 volts, 60 cycles.

For the results shown in Fig. 13, the capacity C_2 was adjusted to exactly neutralize the internal capacity C_1. Under this condition the operation of the thyratron was under the control of the bias potential V_g. With no light on the photocell and the bias at -4.3 volts A.C., the circuit did not operate falsely even with rather wide variations of power supply and temperature.

Curve *A* of Fig. 13 shows the variation of the thyratron plate current with light intensity using the same light scale as in Fig. 11. The "dashed" part of each curve represents the range over which the thyratron was operating in periodic flashes at a frequency less than 60 cycles while the dotted

FIG. 14.

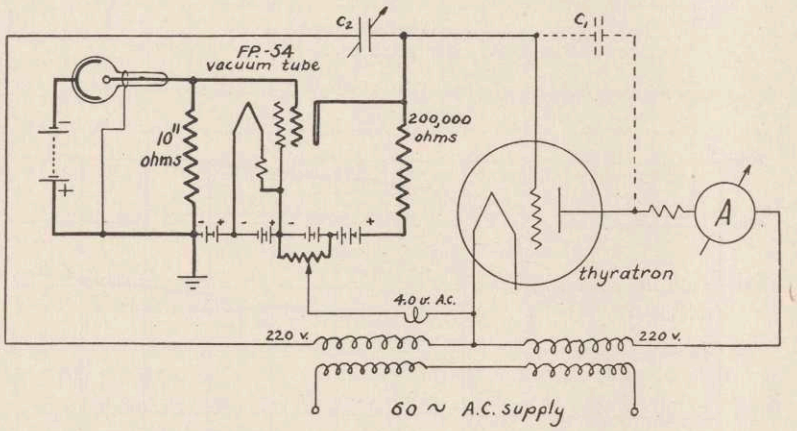

Circuit for Thyratron control using low grid current amplifier *FP*-54.

part represents a transient range which was not stable in the sense that it could be traced. Curve *B* of Fig. 13 shows the response of the thyratron with the grid bias adjusted to within about 0.1 volt of the operating value. Although the circuit worked perfectly over short periods of time with this "trigger" adjustment, operation with such a narrow margin is certainly not recommended. Curve "*C*" is the "1.05" curve of Fig. 11 reproduced for comparison.

The lower limit of photoelectric current which can be used with a good margin of safety is about 10^{-8} ampere. This amount can easily be produced with the light reflected from a

galvanometer mirror. If applications arise in which it is necessary to operate a thyratron on much less than 10^{-8} ampere a vacuum tube amplifier should be used. The photoelectric cell must be designed as so to have a "dark current" which is considerably less than the controlling photoelectric current. Fig. 14 shows a circuit using the General Electric "*FP*-54 low grid current vacuum tube" [5] by which it is theoretically possible to obtain reliable operation of a thyratron with a photoelectric current of 10^{-11} ampere.

A high vacuum photoelectric cell can be used with either the "phase shift" or the "critical potential" method of control with very little change in the general form of the characteristics obtained but with considerable loss in sensitivity.

CHARACTERISTICS OF AN FG-27 THYRATRON.

(a) Static Characteristics.

The static characteristics of an *FG*-27 thyratron were taken using the methods described above and the circuit shown in

FIG. 15.

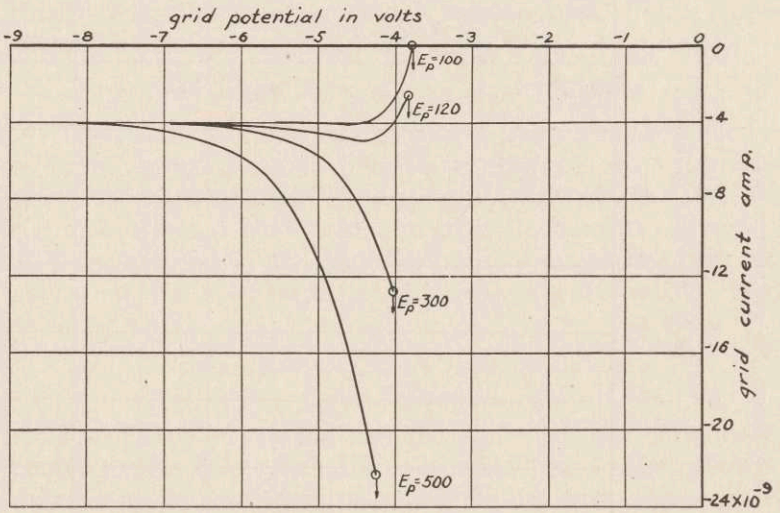

FG-27 thyratron—grid current before discharge.

Fig. 1 The results were very similar in character to those obtained on the *FG*-17 and are shown in Figs. 15 and 16.

[5] Metcalf and Thompson, *Phys. Rev.*, 36, 1489 (1930).

FIG. 16.

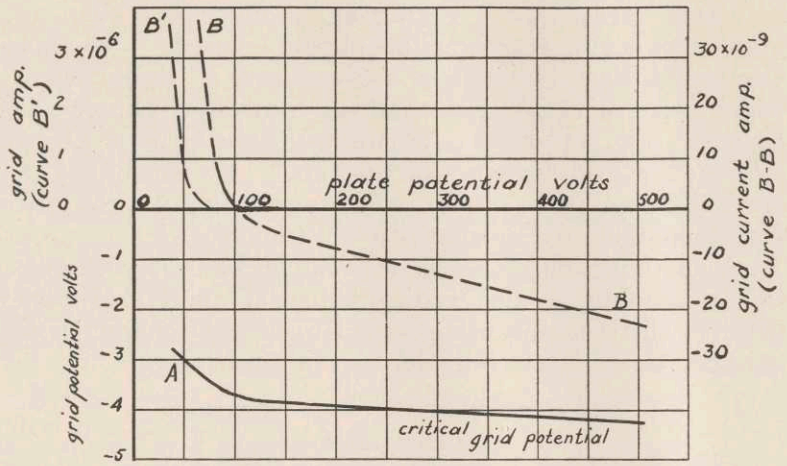

FG-27 thyratron—Grid potential and grid current before discharge at critical point.

FIG. 17.

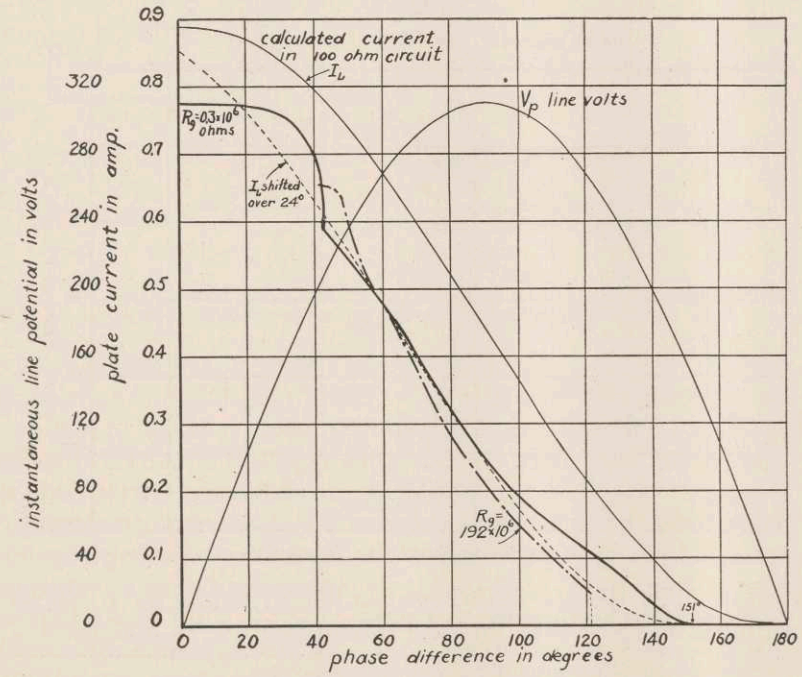

A.C. characteristics of an *FG*-27 thyratron—220 volts, 60 cycles.

By comparing Fig. 15 with Fig. 2 and Fig. 16 with Fig. 5, it is obvious that there are no significant differences between the general forms of these characteristics. The relation between the plate current and the grid current before the discharge began was found to be linear as in the case of the *FG*-17 illustrated by Fig. 3.

(b) Dynamic Characteristics.

The dynamic characteristics of the *FG*-27 also showed a very close similarity to those of the *FG*-17. The curves of Fig. 17 should be compared with those of Fig. 8. The circuit used is shown in Fig. 6. Equation 10 was used to calculate the line current as a function of starting phase using a plate resistance R_p of 100 ohms instead of 400 ohms as above.

Again it will be noticed that the calculated current flow without introducing the time lag hypothesis does not agree with the observations, but if it is assumed that a time of 1.1×10^{-3} sec. is required to start the discharge, the observed and the calculated curves agree fairly well. The fact that this time lag was independent of the plate potential, is demonstrated by the curve shown in Fig. 9.

FG-27 THYRATRON CONTROL WITH A PHOTOELECTRIC CELL.

The results obtained with the *FG*-27 in photoelectric control circuits were so near like those obtained with the *FG*-17 that it is not worth while to reproduce the curves. The only significant fact is that, with the circuit constants adjusted to give approximately the same margins of safety against false operation, the *FG*-27 was found to be less sensitive by a factor of about two.

CHARACTERISTICS OF AN FG-67 THYRATRON.

(a) Static Characteristics.

The *FG*-67 thyratron has the same current carrying capacity as the *FG*-27 but differs in mechanical construction in that both the anode and the cathode are surrounded by the grid and the spacing between the grid and the anode is much less than in the *FG*-27. This mechanical difference causes an increase in the internal capacities of the tube C_0 and C_1 of Fig. 6. The measured values of these capacities were $C_0 = 20 \times 10^{-12}$ farad and $C_1 = 14 \times 10^{-12}$ farad. While

the *FG*-27 and the *FG*-17 were designed as "controlled rectifiers" the *FG*-67 has been designed for "inverter" work. A number of useful inverter circuits are shown by Hull.[1] These circuits and slight modifications of them will undoubtedly find many uses in the physics laboratory where a source of pulsating direct current power is needed.

The static characteristics obtained on an *FG*-67 using the methods outlined above are shown in Figs. 18, 19 and 20.

FIG. 18.

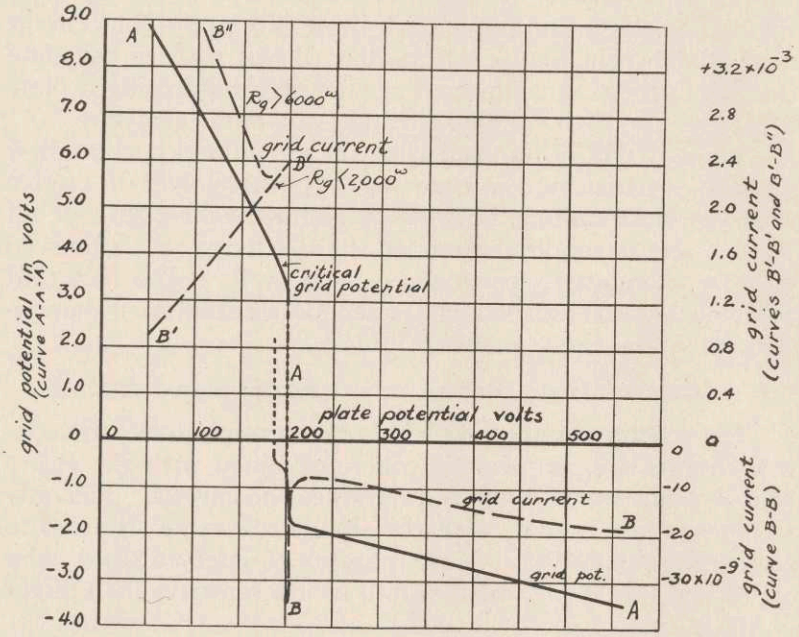

FG-67 thyratron (Condensation temp., 47.5° C.)—Grid potential and grid current at critical point.

Figure 18 shows the critical grid potential and critical grid current as a function of the D.C. line potential. The curves here show a very marked difference when compared with those for the *FG*-17 and *FG*-27 of Figs. 5 and 16. At about 200 volts the critical grid potential suddenly changes from positive to negative values as the line potential is raised and the grid current required to operate the thyratron changes from 2.4×10^{-3} to -8×10^{-9}, a change in magnitude of almost a million. The variation of grid current with grid potential is shown for various plate potentials above 200 volts in Fig. 19.

These curves have much the same general form as those shown in Figs. 2 and 15.

With a plate potential of 160 volts the grid current characteristic is much more complicated. This is shown in Fig. 20.

FIG. 19.

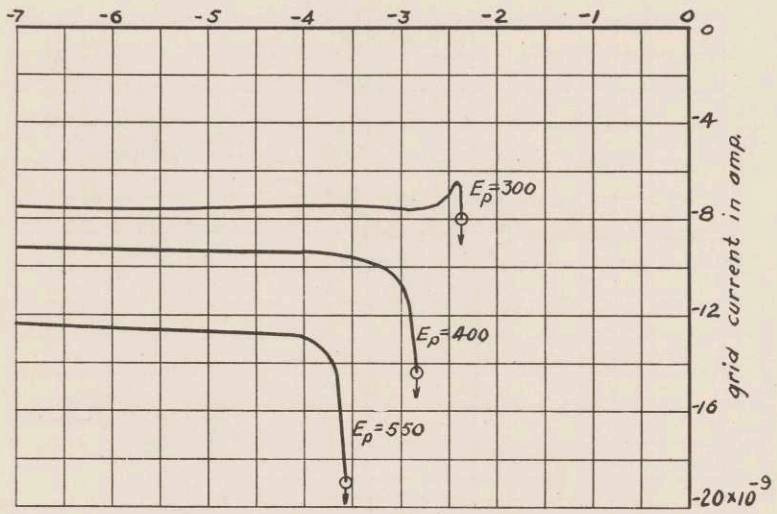

FG-67 thyratron—Grid current before discharge (Condensation temp., 47.5° C.).

With high negative grid potentials the grid current follows the generally expected curve showing the effect of the increase in positive ion current between -2 and -1.5 volts. At -1.5 volts a discharge developed between the *grid and the plate* which resulted in a sudden increase in the grid current from 160×10^{-9} to 0.13×10^{-3}. In spite of this large ion current, a space charge sheath did *not build up around the grid* and the thyratron did not really operate. At -0.2 volt the number of electrons coming from the cathode to the grid was equal to the number of positive ions, making the net current zero. At a grid potential of $+1.5$ a "low voltage discharge" suddenly developed between the grid and the cathode. The characteristic "blue glow" showing the predominance of the 5461 Å, 4358 Å and the 4047 Å lines of the triplet series gradually became stronger with increasing grid potential until at $+4.4$ volts the full discharge in the thyratron took place and a com-

plete sheath formed around the grid which caused it to lose control. With lower line potentials still more complicated forms of the grid current characteristic were found but since a detailed knowledge of these is of no particular value they will not be described.

FIG. 20.

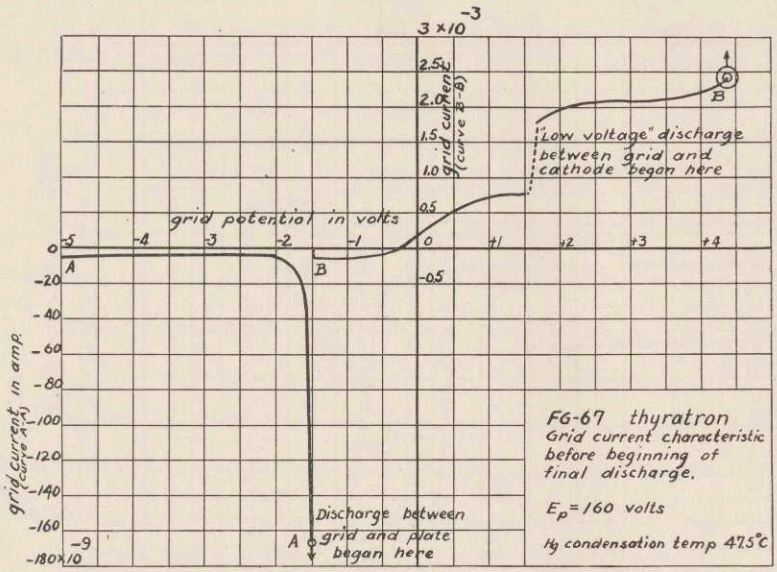

FG-67 thyratron—Grid current before beginning of final discharge—E_p = 160 volts (Condensation temp., 47.5° C.).

Four *FG*-67 thyratrons showed characteristics very similar to those shown above. The plate potential at which the critical grid potential crosses over from positive to negative values is a *function of the condensation temperature.* Figure 21 shows the observed relation between the "cross-over" potential and the condensation temperature as measured by a thermocouple placed in contact with the glass wall of the thyratron directly above the base. With the grid entirely disconnected or "free," the plate potential was raised very slowly until the discharge began. The critical value of plate potential found in this way was equal to the "cross-over" potential shown in Fig. 18.

From the curve of Fig. 21, it is easy to see that a change of temperature of only a few degrees may cause a given thyratron

system to fail to operate unless the grid control circuit is capable of furnishing *milliamperes* of grid current. It was this particular difficulty which prompted the undertaking of this study of thyratrons.

FIG. 21.

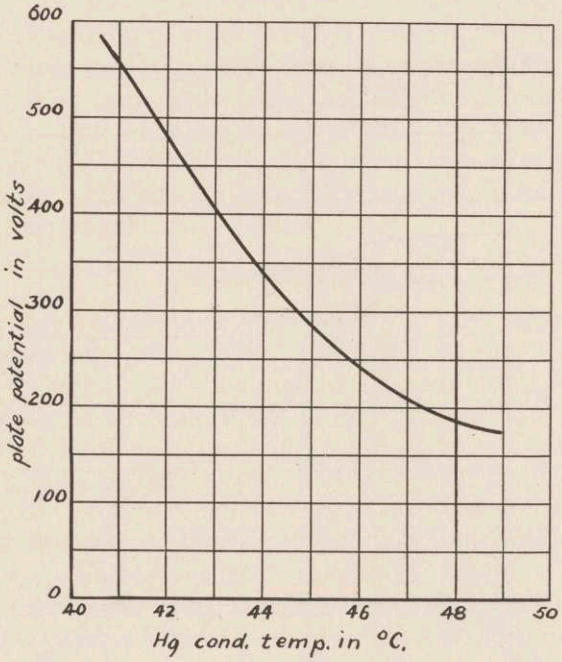

Plate potential for "free grid" operation of an *FG*-67 thyratron as a function of mercury condensation temperature.

The condensation temperature was found to be 25° to 28° C. higher, than the ambient temperature for the *FG*-27 and *FG*-67 thyratrons and about 17° C. higher for the *FG*-17. The ambient temperature was measured with a mercury thermometer at a distance of about three inches. Since all measurements were made in a shielded box 18″ × 18″ × 15″, the air circulation was not as good as it would have been with the tubes unshielded. For applications where only a small power input to the grid is available using the *FG*-67 thyratron with plate voltages between 200 and 500 volts, care must be used to keep the tubes warm enough during use to maintain a condensation temperature between 50° and 60° C.

(b) **Dynamic Characteristics of an FG-67 Thyratron.**

The dynamic characteristics of the *FG*-67 thyratron as a "controlled rectifier" were measured using the methods described above and the results are shown in Fig. 22.

FIG. 22.

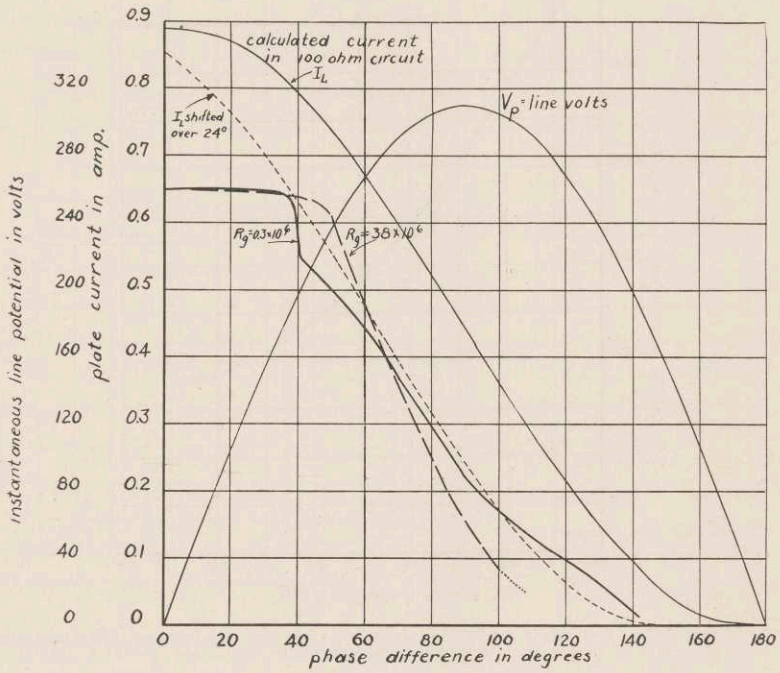

A.C. characteristics of an *FG*-67 thyratron 220 volt, 60 cycles.

Here as in the previous cases the observed curve was better represented by the calculated curve if a time lag of 1.1×10^{-3} sec. was introduced as above. This result in all three cases is so unexpected and so hard to explain even in a qualitative way that there is still some doubt as to whether or not it is the true explanation of the observations. All that can be said for this "time lag hypothesis" is that it does agree with the observations to date. The experiments have not been of a kind, however, that make this conclusion unavoidable. Observations should be taken using an oscillograph, because if it is true that it requires 10^{-3} sec. to start a thyratron, this is just as

important a fact to know in many applications as is the fact that it requires 10^{-4} sec. to stop it and restore control to the grid.

TECHNICAL SUGGESTIONS.

(a) Shielding.

In all thyratron circuits using grid resistances of 10^6 ohms or greater it is well to provide shielding because power circuits in neighboring apparatus can cause oscillations to be superimposed on the normal grid potentials and thus cause uncertain or false operation. This suggestion also applies to "phase shift" circuits, in case the capacities used are of the order of .004 microfarad or less.

(b) Design of a Small Variable Capacity.

For capacities smaller than 50×10^{-6} microfarad, cylindrical condensers were made from brass tubing. The inside cylinder (which was connected to the grid) had an outside diameter of $\frac{3}{8}$ inch and the outer cylinder had an inside diameter of $\frac{5}{8}$ inch. The inner cylinder was made in four sections 5 cm., 10 cm., 15 cm. and 20 cm. in length and supported on a straight vertical rod of hard rubber which was held in a block of sulphur to furnish high insulation between the inner cylinder and the supporting frame. The outer cylinder was insulated by bakelite blocks from its support and arranged so that it could be raised or lowered definite amounts while it was held concentric with respect to the inner cylinder. The main support was connected to the cathode or the ground connection and the outer cylinder connected to the high potential. This construction eliminated any leakage current across the insulators from the "high potential" cylinder to the grid connection. The capacity could be varied by putting in various lengths of the inner cylinder (from 5 cm. to 50 cm.) and also by the movement of the outer cylinder with respect to the inner. The standard formula given in equation (12) which neglects the end effect in a cylindrical condenser was found to hold very well for this condenser.

$$C = \frac{0.2416\, l}{\log_{10} \frac{r_1}{r_2}}. \qquad (12)$$

Where l is the length in cm., r_1 is the inside radius of the outer cylinder and r_2 is the outside radius of the inner cylinder, the capacity C is then given in micro-microfarads.

The cross section of a second condenser used for the very small capacities is shown in Fig. 23.

FIG. 23.

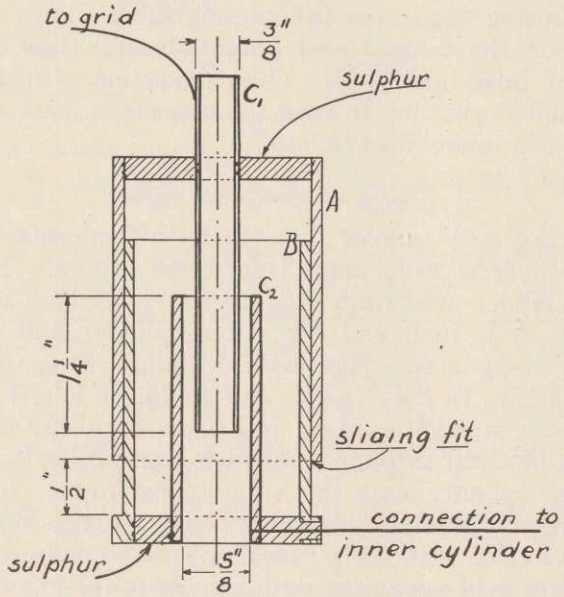

Cylindrical condenser with approximate range 0.5 to 5 $\times$ 10^{-12} farad.

This condenser is made of four pieces of brass tubing, C_1 the inner cylinder, C_2 the outer cylinder of the condenser and A and B the sliding support. The maximum capacity obtained with this condenser was about 5 $\times$ 10^{-12} farad and served very satisfactorily for the neutralizing condenser C_2 in Fig. 12.

(c) High Resistances.

High resistances made using Higgens India ink have been described in a previous paper,[3] but it is perhaps necessary to call attention to the fact that such resistances do not follow Ohm's law with high potentials unless the line is made sufficiently broad. Resistances made with "Aquadag" [6] are used

[6] A graphite product of the Acheson Oildag Co. of Port Huron, Mich.

by some for the production of high resistances but the author has not yet given this resistance material a test.

CONCLUSION.

Although the characteristics of thyratrons shown in this paper do not cover all of the important details of thyratron operation, it is hoped that the information given will be of value to those who have already tried to make use of the thyratron and have run into minor difficulties, and also serve further to introduce the thyratron and encourage physicists to make use of this new and very valuable thermionic device, which has so many possible applications in the present day scientific laboratory.

Since writing of this article I have found certain interesting facts concerning the early development of the thyratron which are not well known. During the year 1913 Prof. George W. Pierce carried out a series of very interesting investigations with gas filled tubes containing a cathode, grid, and anode. These tubes were used as amplifiers and detectors in somewhat the same way as the tubes described by Eugen Reisz (E. T. Z. 34, 1356 (1913)). The theory of operation, as understood at that time, is given in considerable detail in the three United States patents 1,112,655; 1,087,180 and 1,112,549 all of which were applied for in the second half of 1913. Very early in the year 1914, Prof. Pierce discovered the "thyratron properties" of these gas filled three-electrodes tubes much as we know them today and filed an application for a patent on March 11, 1914, in which he described numerous circuits including one using a selenium cell about which he writes: "This form of device is very sensitive and it has been found that the light of a candle across a room focused on the selenium cell is sufficient to effect the control of several amperes in the controlled circuit." (U. S. Patent 1,450,749.)

PRINTED IN THE U. S. A.

LANCASTER PRESS, INC.
LANCASTER, PA.